A Ferrocene-Containing Carbohydrate Surfactant: Thermotropic and Lyotropic Phase Behavior

Bertrand Donnio,[†,§] John M. Seddon,*[,‡] and Robert Deschenaux*[,†]

Institut de Chimie, Université de Neuchâtel, Avenue de Bellevaux 51, Case postale 2, 2007 Neuchâtel, Switzerland, and Department of Chemistry, Imperial College, London WS7 2AY, England

Received February 17, 2000

A ferrocene-containing carbohydrate surfactant has been synthesized and shown by polarized optical microscopy, differential scanning calorimetry, and X-ray diffraction to exhibit both thermotropic and lyotropic liquid-crystalline phase behavior. This new class of materials should prove useful for the design of redox-active lyotropic liquid crystals, allowing fine electrochemical control of the phase structure and symmetry.

Introduction

Little attention has been devoted to the design and study of amphiphilic metallomesogens[1] (metallomesogen = metal-containing liquid crystal). Early examples concerned alkali-metal soaps,[2] carboxylated copper phthalocyanines,[3] and cobalt annelides.[4] Parallel to investigations devoted to thermotropic metallomesogens, further metal-containing lyotropic liquid crystals have been described: octahedral surfactant complexes of chromium,[5a] cobalt,[5a] and ruthenium,[5b,c] oxovanadium-based surfactants,[6] and an ionic silver complex of a macrocyclic ligand.[7] Finally, a few other lyotropic metallo-organic systems have been recently reported, i.e., one-chain octahedral nickel complexes,[8] double-chain octahedral cobalt complexes,[9] and chiral dinuclear chromium complexes.[10]

Metal-based lyotropic liquid crystals are of interest from structural (the presence of the metal−ligand complex offers the opportunity to design surfactants with unusual shapes and geometries with respect to conventional organic structures) and activity (catalysis, magnetism, redox behavior) aspects. The choice of the metal-containing subunit is of prime importance if specific properties are to be exploited.

Ferrocene has proved to be a valuable unit for constructing thermotropic liquid crystals[11−13] and Langmuir and Langmuir−Blodgett films:[14] the molecular organization could be controlled as a function of the nature, number, and position of the substituents located on the ferrocene core. In view of these investigations, we envisaged the possibility of using ferrocene to design organometallic-based amphiphilic liquid crystals. Such systems are attractive for further exploration of the capability of ferrocene to be used as a molecular unit for the construction of ordered supramolecular materials. Furthermore, the finding that electron transfer can be exploited in the ferrocene−ferrocenium redox system to generate mesomorphism[15] and vesicle formation[16] is of interest for the elaboration of switchable lyotropic liquid crystals. Finally, the study of new lyotropic liquid crystals is attractive considering their possible uses, e.g., for the fabrication of nanostructured materials[17] and as models for cell membranes.[18]

* Corresponding author. For R.D. Fax: (++41) 32 718 25 11. E-mail: robert.deschenaux@ich.unine.ch.
† Université de Neuchâtel.
‡ Imperial College.
§ Current address: Institut de Physique et Chimie des Matériaux de Strasbourg, Groupe des Matériaux Organiques, 23 Rue de Loess, 67037 Strasbourg Cedex, France.

(1) (a) Collinson, S. R.; Bruce, D. W. In *Transition Metals in Supramolecular Chemistry*; Sauvage, J.-P., Ed.; Wiley: Chichester, 1999; pp 285−369. (b) Donnio, B.; Bruce, D. W. *Struct. Bond*. **1999**, *95*, 193. (c) Bruce, D. W. In *Inorganic Materials*, 2nd ed.; Bruce, D. W., O'Hare, D., Eds.; Wiley: Chichester, 1997; pp 429−522. (d) Neve, F. *Adv. Mater*. **1996**, *8*, 277.
(2) Skoulios, A. *Adv. Colloid Interface Sci* **1967**, *1*, 79.
(3) (a) Gaspard, S.; Hochapfel, A.; Viovy, R. *C. R. Hebd. Seances Acad. Sci., Ser. C* **1979**, *289*, 387. (b) Usolt'seva, N. V.; Maizlish, V. E.; Bykova, V. V.; Anan'eva, G. A.; Shaposhnikov, G. P.; Kormilitsyn, N. M. *Zh. Fiz. Khim*. **1989**, *63*, 2931.
(4) Le Moigne, J.; Simon, J. *J. Phys. Chem*. **1980**, *84*, 170.
(5) (a) Bruce, D. W.; Denby, I. R.; Tiddy, G. J. T.; Watkins, J. M. *J. Mater. Chem*. **1993**, *3*, 911. (b) Bruce, D. W.; Holbrey, J. D.; Tajbakhsh, A. R.; Tiddy, G. J. T. *J. Mater. Chem*. **1993**, *3*, 905. (c) Holbrey, J. D.; Tiddy, G. J. T.; Bruce, D. W. *J. Chem. Soc., Dalton Trans*. **1995**, 1769.
(6) Zhu, S. S.; Swager, T. M. *Adv. Mater*. **1995**, *7*, 280.
(7) Neve, F.; Ghedini, M.; De Munno, G.; Levelut, A.-M. *Chem. Mater*. **1995**, *7*, 688.
(8) Fallis, I. A.; Griffiths, P. C.; Hibbs, D. E.; Hursthouse, M. B.; Winnington, A. L. *Chem. Commun*. **1998**, 665.
(9) Jaeger, D. A.; Reddy, V. B.; Arulsamy, N.; Bohle, D. S.; Grainger, D. W.; Berggren, B. *Langmuir* **1998**, *14*, 2589.
(10) Imae, T.; Ikeda, Y.; Iida, M.; Koine, N.; Kaizaki, S. *Langmuir* **1998**, *14*, 5631.
(11) Review on low-molar-mass ferrocene-containing thermotropic liquid crystals: Deschenaux, R.; Goodby, J. W. In *Ferrocenes: Homogeneous Catalysis, Organic Synthesis, Materials Science*; Togni, A., Hayashi, T., Eds.; VCH: Weinheim, 1995; pp 471−495.
(12) Ferrocene-containing side-chain liquid-crystalline polymers: (a) Deschenaux, R.; Jauslin, I.; Scholten, U.; Turpin, F.; Guillon, D.; Heinrich, B. *Macromolecules* **1998**, *31*, 5647. (b) Deschenaux, R.; Turpin, F.; Guillon, D. *Macromolecules* **1997**, *30*, 3759. (c) Deschenaux, R.; Izvolenski, V.; Turpin, F.; Guillon, D.; Heinrich, B. *Chem. Commun*. **1996**, 439. (d) Deschenaux, R.; Kosztics, I.; Scholten, U.; Guillon, D.; Ibn-Elhaj, M. *J. Mater. Chem*. **1994**, *4*, 1351.
(13) Ferrocene-containing liquid-crystalline dendrimers: (a) Deschenaux, R.; Serrano, E.; Levelut, A.-M. *Chem. Commun*. **1997**, 1577. (b) Dardel, B.; Deschenaux, R.; Even, M.; Serrano, E. *Macromolecules* **1999**, *32*, 5193.
(14) Deschenaux, R.; Megert, S.; Zumbrunn, C.; Ketterer, J.; Steiger, R. *Langmuir* **1997**, *13*, 2363, and references therein.
(15) (a) Deschenaux, R.; Schweissguth, M.; Levelut, A.-M. *Chem. Commun*. **1996**, 1275. (b) Deschenaux, R.; Schweissguth, M.; Vilches, M.-T.; Levelut, A.-M.; Hautot, D.; Long, G. L.; Luneau, D. *Organometallics* **1999**, *18*, 5553.
(16) Wang, K.; Munoz, S.; Zhang, L.; Castro, R.; Kaifer, A. E.; Gokel, G. W. *J. Am. Chem. Soc.* **1996**, *118*, 6707.

10.1021/om0001568 CCC: $19.00
Publication on Web 07/06/2000

Chart 1

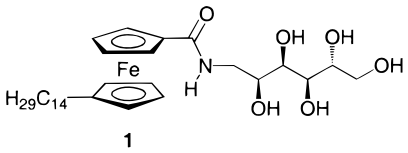

1

Scheme 1[a]

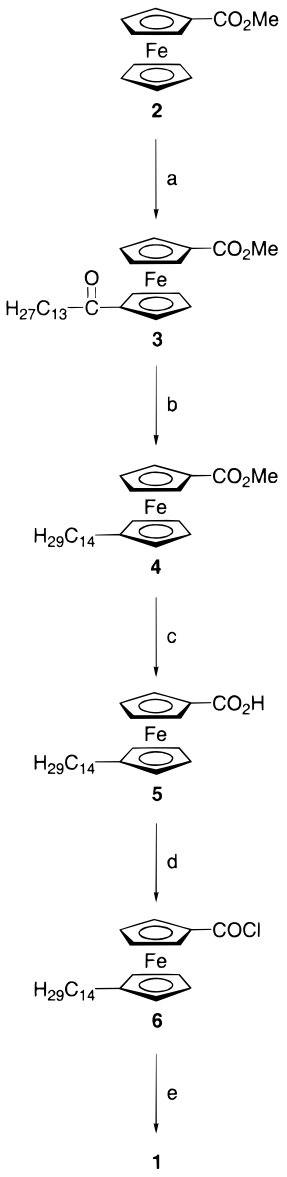

[a] (a) $C_{14}H_{29}COCl$, Zn, $AlCl_3$, CH_2Cl_2, 0 °C, 79%. (b) Zn, $HgCl_2$, H_2O, concentrated HCl, toluene, reflux, 4 h, 96%. (c) KOH, EtOH, reflux, 4 h, 97%. (d) Oxalyl chloride, pyridine, CH_2Cl_2, reflux, 5 h, 100%. (e) 1-Amino-1-deoxy-D-sorbitol, 4-(dimethylamino)pyridine, DMF−CH_2Cl_2, 80 °C for 3 h and then rt for 24 h, 36%.

We report, herein, the synthesis and thermotropic and lyotropic (amphotropic) liquid-crystalline behavior of the amphiphilic ferrocene derivative **1** (Chart 1), which is substituted at the 1,1′-positions by a sugar moiety (1-amino-1-deoxy-D-sorbitol) and a long alkyl chain (14 carbon atoms). The substituents, in particular the sugar framework, were selected in view of successful investigations performed with organic-type amphiphilic carbohydrate surfactants.[19,20]

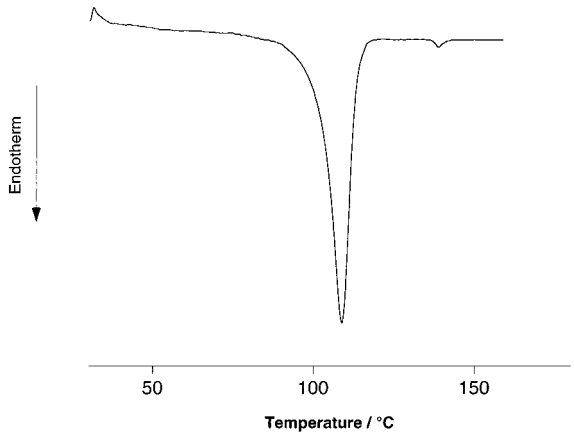

Figure 1. Differential scanning calorimetry thermogram of **1** recorded during the first heating run.

Results and Discussion

Synthesis. The preparation of **1** is described in Scheme 1. Carbomethoxyferrocene (**2**)[14] was acylated with myristoyl chloride under Friedel−Crafts reaction conditions to give **3**, the reduction of which gave the alkyl derivative **4**. Acid intermediate **5** was obtained by hydrolysis of the methyl ester function of **4** under alkaline alcoholic conditions. Treatment of **5** with oxalyl chloride led to the corresponding acid chloride **6**. Finally, condensation of **6** with 1-amino-1-deoxy-D-sorbitol, adapting a literature procedure,[21] gave the targeted ferrocene derivative **1**.

Liquid-Crystalline Properties. The mesomorphic properties of **1** were investigated by a combination of polarized optical microscopy (POM), differential scanning calorimetry (DSC), and X-ray diffraction (XRD).

(a) Thermotropic Liquid-Crystalline Behavior. Two endotherms were detected by DSC at 98 ($\Delta H = 53.7$ kJ mol^{-1}) and 137 °C ($\Delta H = 0.4$ kJ mol^{-1}) during the first heating run (Figure 1) and were indicative of enantiotropic liquid-crystalline behavior. On cooling, only one exotherm was registered at 137 °C ($\Delta H = 0.4$ kJ mol^{-1}), revealing an absence of crystallization of the sample under the applied experimental conditions (10 °C min^{-1}). During the second heating run, an endotherm was obtained at 137 °C ($\Delta H = 0.4$ kJ mol^{-1}), which confirmed the reversibility of the transition.

POM investigations supported the DSC data: the initial crystalline sample melted at 98 °C, giving rise to a birefringent fluid which cleared at 137 °C. Cooling of the sample from the isotropic liquid provided a liquid-

(17) (a) Deng, H.; Gin, D. L.; Smith, R. C. *J. Am. Chem. Soc.* **1998**, *120*, 3522. (b) Smith, R. C.; Fischer, W. M.; Gin, D. L. *J. Am. Chem. Soc.* **1997**, *119*, 4092. (c) Gray, D. H.; Hu, S.; Juang, E.; Gin, D. L. *Adv. Mater.* **1997**, *9*, 731.

(18) (a) Goodby, J. W. *Liq. Cryst.* **1998**, *24*, 25. (b) Auzély-Velty, R.; Benvegnu, T.; Plusquellec, D.; Mackenzie, G.; Haley, J. A.; Goodby, J. W. *Angew. Chem. Int. Ed.* **1998**, *37*, 2511. (c) Ringsdorf, H.; Schlarb, B.; Venzmer, J. *Angew. Chem., Int. Ed. Engl.* **1988**, *27*, 113.

(19) (a) Tschierske, C. *J. Mater. Chem.* **1998**, *8*, 1485. (b) Blunk, D.; Praefcke, K.; Vill, V. In *Handbook of Liquid Crystals Vol. 3: High Molecular Weight Liquid Crystals*; Demus, D., Goodby, J. W., Gray, G. W., Spiess, H.-W., Vill, V., Eds.; Wiley-VCH: Weinheim, 1998; pp 305−340. (c) Sakya, P.; Seddon, J. M.; Templer, R. H. *J Phys. II Fr.* **1994**, *4*, 1311.

(20) (a) Jeffrey, G. A.; Wingert, L. M. *Liq. Cryst.* **1992**, *12*, 179. (b) Prade, H.; Miethchen, R.; Vill V. *J. Prakt. Chem.* **1995**, *337*, 427.

(21) Borisch, K.; Diele, S.; Göring, P.; Müller, H.; Tschierske, C. *Liq. Cryst.* **1997**, *22*, 427.

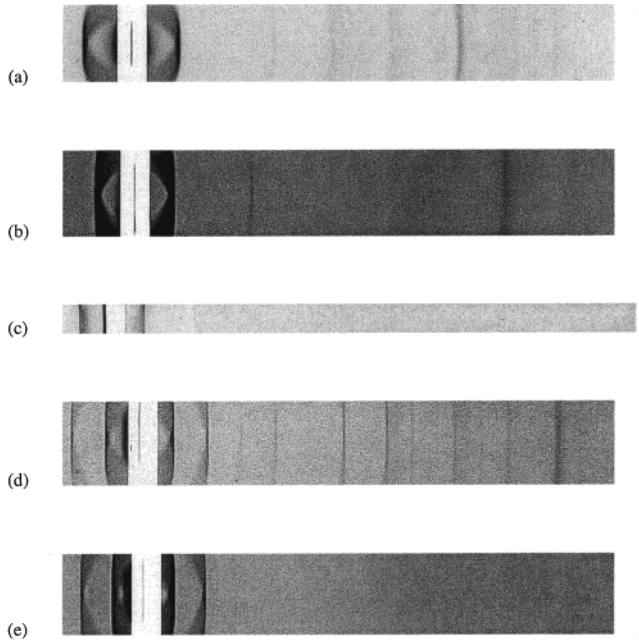

Figure 2. X-ray powder patterns of **1**: (a) the crystalline phase of the initial compound at 26 °C; (b) a gel-like (hexatic) smectic phase observed for the dry compound upon cooling the smectic A phase below 25 °C; (c) the smectic A phase observed above 100 °C; (d) the crystalline lamellar phase observed for the sample in water upon cooling the L_α phase below 31 °C; and (e) the fluid lamellar L_α phase at 42 °C, after heating above the Krafft point of 57 °C. The center of the patterns is marked (except for c) by the direct beam, within the backstop, which is offset toward the left-hand side of the figure. The patterns extend on the right-hand side to spacings of approximately 3.5 Å (2.3 Å for c, which was obtained using a different Guinier camera).

crystalline phase characterized by fanlike and homeotropic textures. From these observations, the mesophase was identified as a smectic A phase.

XRD measurements of the initial crystalline phase at 26 °C (Figure 2a) showed strong first-order and weak third-order Bragg peaks, with a layer periodicity of 33.0 Å. The wide-angle pattern consisted of a number of reflections, the strongest one being at a spacing of 4.80 Å. On heating above the melting point at 98 °C and cooling back to room temperature, quite a different diffraction pattern was obtained (Figure 2b). In the low-angle region, a strong first-order and weaker third- and fifth-order layer reflections were observed, with a periodicity of 39.6 Å. The wide-angle pattern consisted of a single, slightly broadened, line at 4.20 Å, plus a region of diffuse scatter in the region of 5.7 Å. The former feature is characteristic of gel phases of surfactants, where the alkyl chains, within a layer, are arranged in a two-dimensional hexagonal lattice, and undergo rapid long axis rotation (such phases are analogous to the hexatic smectic phases of thermotropic mesogens). The diffuse scattering around 5.7 Å presumably arises from a disordered lateral packing of the ferrocene−carbohydrate headgroups. For temperatures between 98 and 137 °C, the pattern (Figure 2c) changed to a single sharp line in the low-angle region and a very diffuse band in the wide-angle region (not clearly visible in Figure 2c). This diffraction pattern is typical of a smectic A phase (it would also be consistent with a

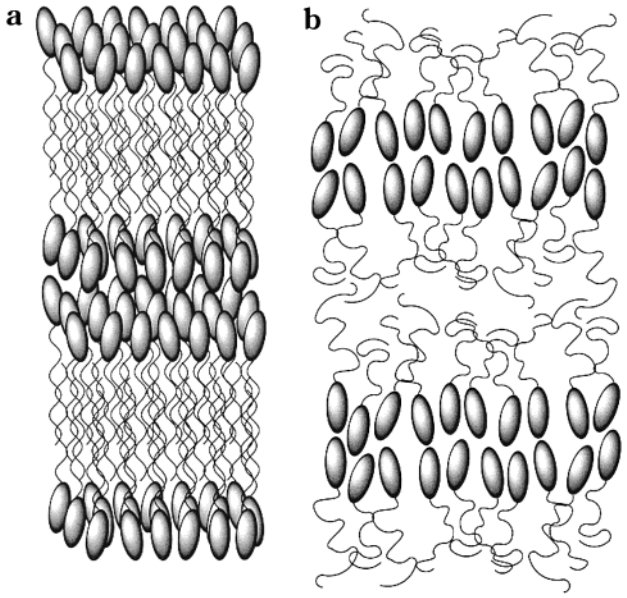

Figure 3. Possible molecular organizations of **1** within the smectic A phase: (a) the aliphatic chains are interdigitated, and (b) microphase separation of the alkyl chains and sugar moieties.

smectic C phase, but the optical texture ruled out this possibility). A *d*-layer spacing of 37.7 Å was found at 105 °C, leading to a d/L ratio of 1.13 (from Corey−Pauling−Koltun (CPK) space-filling molecular models, an approximate molecular length L of 33.5 Å was estimated for **1** in its fully extended conformation).

Two models can be postulated to explain the organization of **1** within the smectic A phase.[22−24] In the first model (Figure 3a),[22] the aliphatic chains are interdigitated and placed in the interior of the layers, whereas the sugar moieties self-assemble in the outer regions of the bilayers. Partial interpenetration of the sugar units can also be envisaged. In the second model (Figure 3b),[23] there is a microphase separation of the alkyl chains and sugar moieties into a fluid bilayer: both the alkyl chains and carbohydrate residues form a disordered packing array, the carbohydrate groups being held together through H-bonds. Study of homologous series of **1** (i.e., by varying the alkyl chain length and the polar headgroup) should allow us to distinguish between the two models.

(b) Lyotropic Liquid-Crystalline Behavior. The lyotropic behavior of **1** in water was first investigated by POM applying two techniques. In the first method, contact preparations were obtained by melting (with the heating stage of the microscope) a small amount of the sample sandwiched between a microscope slide and a cover slip. The melt was cooled to room temperature, and water was introduced between the slide and the cover slip: a concentration gradient from pure sample (center of the preparation) to pure water (edge of the cover slip) was obtained. In the second method, a dilute

(22) Goodby, J. W.; Haley, J. A.; Mackenzie, G.; Watson, M. J.; Plusquellec, D.; Ferrières, V. *J. Mater. Chem.* **1995**, *5*, 2209.
(23) Goodby, J. W.; Watson, M. J.; Mackenzie, G.; Kelly, S. M.; Bachir, S.; Bault, P.; Godé, P.; Goethals, G.; Martin, P.; Ronco, G.; Villa, P. *Liq. Cryst.* **1998**, *25*, 139.
(24) (a) Paleos, C. M.; Tsiourvas, D. *Angew. Chem., Int. Ed. Engl.* **1995**, *34*, 1696. (b) Paleos, C. M.; Tsiourvas, D. *Adv. Mater.* **1997**, *9*, 695.

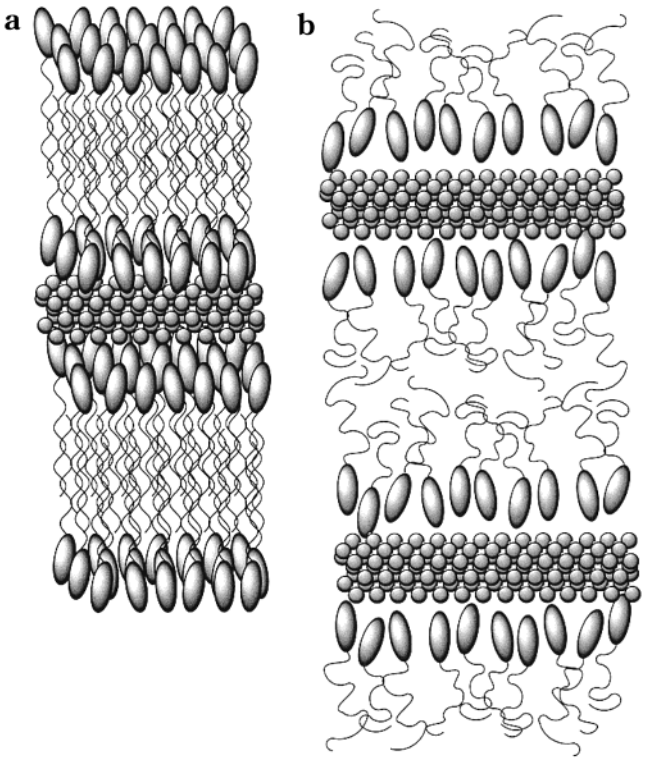

Figure 4. Possible molecular organizations of **1** within the L_α phase: (a) fluid bilayers with interdigitated aliphatic chains, (b) fluid bilayers without chain interdigitation.

aqueous solution of **1** was slowly evaporated. These experiments, which were conducted between 60 and 70 °C, indicated the formation of a liquid-crystalline phase characterized by the formation of oily streaks and Myelin figures.[19a,25] These observations were indicative of the formation of a L_α phase, in agreement with the structure of **1**.

By DSC (hydrated sample; **1**, 7 mg; water, 30 mg), an endotherm was observed at 57 °C ($\Delta H = 46$ kJ mol^{-1}) during the first heating run. This transition corresponded to the Krafft point (formally defined as the temperature at which the surfactant solubility equals the critical micelle concentration), with a simultaneous penetration of water into the sample and melting of the crystal lattice leading to the formation of the liquid-crystalline phase; in other words, this transition reflected the crystal-to-lyotropic liquid-crystal phase transition. Cooling of the sample and reheating gave a transition temperature at 39 °C ($\Delta H = 44$ kJ mol^{-1}); the two different temperatures detected during the first and second heating runs indicated that the structure of the crystalline phase obtained during the cooling run was different from that of the native sample.

XRD investigations clarified the nature of these phase transitions. The initial crystalline phase was unchanged upon addition of water below the Krafft temperature of 57 °C (diffraction pattern not shown). Heating above 57 °C and cooling back to room temperature led to the formation of a different crystalline lamellar phase (Figure 2d), with sharp first-, second-, third-, fourth-, and sixth-order low-angle layer reflections with a periodicity of 45.6 Å. A number of wide-angle reflections were observed, confirming that this is a crystalline lamellar phase. For temperatures above 57 °C (or above 39 °C on subsequent heating scans, which is the melting point of the 45.6 Å crystalline lamellar phase), the pattern (Figure 2e) consisted of sharp first- and second-order low-angle reflections and only weak diffuse scattering in the wide-angle region. This diffraction pattern is characteristic of a disordered smectic (fluid lamellar L_α) phase. The *d*-layer spacing was found to be 50.0 Å at 60 °C. Therefore, a 12.3 Å difference in layer thickness was obtained between the thermotropic and lyotropic mesophases. This increase of the layer thickness is attributed to the incorporation of water molecules between the layers of **1** (in the thermotropic phase).

Chart 2

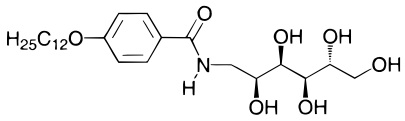

I

Two models can be envisaged for the structure of the L_α phase derived from Figures 3a and 3b, respectively. In the first case (Figure 4a), the alkyl chains remain interdigitated as the water penetrates the polar groups. This model would imply a rather large interfacial area per molecule for the headgroups. The second possibility is that the lamellar L_α phase consists of fluid surfactant bilayers separated by thin layers of water (Figure 4b). A more detailed structural study is required to distinguish conclusively between these two possibilities. In any event, assuming that the surfactant layer remains at the same thickness of approximately 38 Å, which it has in the dry smectic A phase, this would imply a water layer thickness of 12 Å in the fully hydrated L_α phase.

Comparison of the thermotropic properties of **1** with those reported for the ferrocene-free analogue **I** (Cr → S_A: 182 °C; S_A → I: 250 °C)[19a,21] (Chart 2) revealed that replacement of the benzene ring by the ferrocene unit led to a decrease of the clearing point, i.e., to a destabilization of the liquid-crystalline phase (the influence of the alkyl chain length, 14 carbon atoms for **1** and 12 carbon atoms for **I** can be neglected). This behavior can be explained taking into account the three-dimensional structure of the ferrocene moiety, which acts as a spacer (with respect to the two-dimensional structure of the benzene ring), removing the molecular units from each other, resulting in a lowering of the intermolecular interactions. This result is in agreement with literature data reported for ferrocene-containing thermotropic liquid crystals[11] and for ferrocene-based Langmuir and Langmuir−Blodgett films.[14] It is noteworthy that despite its bulkiness, the ferrocene unit did not completely disrupt the H-bonded network either in the bulk (thermotropic behavior) or in solution (lyotropic behavior), the consequence of which would have been suppression of the mesomorphic character of **1**. Furthermore, it is interesting to point out that the nature of the ferrocene core can adjust to the correct hydrophilic−hydrophobic balance, which is essential for amphotropic behavior to occur.

Conclusion

Careful derivatization of the ferrocene core with a sugar moiety and a long alkyl chain led to an am-

(25) Fuhrhop, J.-H.; Helfrich, W. *Chem. Rev.* **1993**, *93*, 1565.

phiphilic compound that showed thermotropic and lyotropic liquid-crystalline phase behavior. These results are of interest with the view to developing redox-active lyotropic systems and metal-based catalytically active mesoporous solids[26] as elegantly illustrated from an amphiphilic ruthenium complex.[27]

Experimental Section

Materials. CH_2Cl_2 (P_2O_5, under N_2) was distilled prior to use. Oxalyl chloride (Fluka, purum), pyridine (Fluka, puriss p.a.), 4-(dimethylamino)pyridine (Fluka, purum), myristoyl chloride (Aldrich, 97%), 1-amino-1-deoxy-D-sorbitol (Aldrich, 98%), anhydrous $AlCl_3$ (Fluka, puriss p.a.), $LiAlH_4$ (Fluka, puriss), Zn (Fluka, purum), and $HgCl_2$ (Merck) were used as received. Column chromatography: silica gel 60 (0.060−0.200 mm, SDS). Carbomethoxyferrocene (**2**) was prepared following a literature procedure.[14] The syntheses of **1** and **3** were carried out under nitrogen. Abbreviation: 4-(dimethylamino)pyridine = DMAP; column chromatography = CC.

Techniques. NMR spectra: Varian Gemini 200 BB (200 MHz) or Brucker AMX-400 (400 MHz) spectrometer; solvent as internal reference. IR spectra: Perkin-Elmer 1720 FT-IR spectrometer. Mass spectra (ESI, Na): Finnigan LCQ. Transition temperatures (onset point) and enthalpies: differential scanning calorimeter Mettler DSC 30 connected to a Mettler TA 4000 processor, under N_2, at a rate of 10 °C min^{-1}; data treatment used Mettler TA72.2/.5 Graphware; for hydrated samples, the amphiphile mass was typically 7 mg and the water mass 30 mg. Optical studies: Zeiss-Axioscop polarizing microscope equipped with a Linkam-THMS-600 variable-temperature stage, under N_2. X-ray diffraction: Guinier camera (Huber Diffraktionstechnik) operating with Cu $K\alpha_1$ radiation (λ = 1.5405 Å). Melting points (uncorrected) of the intermediates: Büchi 510 instrument. Elemental analyses: Mikroelementaranalytisches Laboratorium Ciba (Marly, Switzerland).

1-Carbomethoxy-1′-tetradecanoylferrocene (3). Powdered zinc (5.36 g, 82.0 mmol) and $AlCl_3$ (1.64 g, 12.3 mmol) were added to a stirred solution of **2** (2.0 g, 8.2 mmol) in CH_2Cl_2 (60 mL) cooled to 0 °C. Myristoyl chloride (2.3 g, 9.3 mmol) in CH_2Cl_2 (40 mL) was added dropwise to the suspension, which was stirred at 0 °C for 3 h. The mixture was allowed to warm to room temperature. The solid was recovered by filtration and washed thoroughly with CH_2Cl_2. The organic phase was hydrolyzed with water (100 mL), washed with a dilute $NaHCO_3$ solution to neutral pH, and dried ($MgSO_4$). The solvent was evaporated to dryness. Purification of the solid residue by CC (CH_2Cl_2) and crystallization (EtOH) gave pure **3** (2.96 g, 79%). Mp: 68 °C. ^{1}H NMR (200 MHz, $CDCl_3$) δ: 0.88 (t, 3 H, CH_3), 1.30 (m, 20 H, $(CH_2)_{10}$), 1.64 (m, 2 H, CH_2), 2.68 (t, 2 H, $COCH_2$), 3.82 (s, 3 H, CO_2CH_3), 4.41 (t, 2 H, HCp), 4.50 (t, 2 H, HCp), 4.79 (t, 2 H, HCp), 4.81 (t, 2 H, HCp). ^{13}C NMR (100 MHz, $CDCl_3$) δ: 14.17, 22.74, 24.39, 29.42, 29.60, 29.71, 31.96, 39.95, 51.82, 70.74, 71.54, 72.69, 72.83, 73.40, 80.44, 171.00, 203.89. Anal. Calcd for $C_{26}H_{38}O_3Fe$ (454.43): C, 68.72; H, 8.43. Found: C, 68.18; H, 8.43.

1-Carbomethoxy-1′-tetradecylferrocene (4). A mixture of powdered zinc (10.36 g, 0.16 mol), $HgCl_2$ (720 mg, 2.65 mmol), water (20 mL), and concentrated HCl (4 mL) was stirred at room temperature for 5 min. The aqueous phase was removed and replaced by water (35 mL) and concentrated HCl (16 mL). A solution of **3** (1.2 g, 2.64 mmol) in toluene (40 mL) was added. The suspension was stirred under reflux for 4 h. The mixture was cooled to room temperature. The organic phase was recovered, diluted with toluene (100 mL), washed with water to neutral pH, dried ($MgSO_4$), and evaporated to dryness. Purification of the residue by CC (CH_2Cl_2) gave pure **4** (1.12 g, 96%) as a red oil, which slowly solidified. Mp: 29 °C. ^{1}H NMR(200 MHz, $CDCl_3$) δ: 0.88 (t, 3 H, CH_3), 1.34 (m, 24 H, $(CH_2)_{12}$), 2.24 (t, 2 H, $CpCH_2$), 3.79 (s, 3 H, CO_2CH_3), 4.07 (s, 4 H, HCp), 4.33 (t, 2 H, HCp), 4.72 (t, 2 H, HCp). ^{13}C NMR (100 MHz, $CDCl_3$) δ: 14.18, 22.76, 28.58, 29.49, 29.56, 29.62, 29.74, 31.14, 31.98, 51.45, 68.87, 69.74, 70.61, 71.54, 71.80, 91.14, 172.06. Anal. Calcd for $C_{26}H_{40}O_2Fe$ (440.45): C, 70.90; H, 9.15. Found: C, 70.80; H, 9.21.

1-Carboxy-1′-tetradecylferrocene (5). A solution of **4** (1.0 g, 2.3 mmol) and KOH (746 mg, 13.3 mmol) in EtOH (50 mL) was stirred under reflux for 4 h. The solution was cooled to room temperature and poured onto a stirred ice/water mixture. Concentrated HCl was added slowly to acid pH. The solid which precipitated was recovered by filtration and washed thoroughly with water. Crystallization (EtOH) gave pure **5** (940 mg, 97%). Mp: 59 °C. ^{1}H NMR (200 MHz, $CDCl_3$) δ: 0.88 (t, 3 H, CH_3), 1.25 (m, 22 H, $(CH_2)_{11}$), 1.46 (m, 2 H, CH_2), 2.25 (t, 2 H, $CpCH_2$), 4.19 (s, 4 H, HCp), 4.45 (t, 2 H, HCp), 4.82 (t, 2 H, HCp). ^{13}C NMR (100 MHz, $CDCl_3$) δ: 14.11, 22.68, 28.32, 29.36, 29.52, 29.63, 29.69, 31.05, 31.92, 69.24, 69.99, 70.18, 71.07, 72.49, 91.26, 178.37. Anal. Calcd for $C_{25}H_{38}O_2Fe$ (426.42): C, 70.42; H, 8.98. Found: C, 70.37; H, 8.97.

Ferrocenylcarbonyl Chloride (6). A solution of **5** (600 mg, 1.41 mmol), oxalyl chloride (1.79 g, 14.1 mmol), and pyridine (5 drops) in CH_2Cl_2 (50 mL) was stirred under reflux for 5 h (in the dark) and cooled to room temperature. The solution was concentrated to dryness, and the solid residue was extracted several times with hot petroleum ether (bp = 80−120 °C). Combination of the organic extracts and evaporation to dryness gave **6** (626 mg, 100%), which was used without further purification. Mp: 47 °C. ^{1}H NMR (200 MHz, $CDCl_3$) δ: 0.89 (t, 3 H, CH_3), 1.36 (m, 24 H, $(CH_2)_{12}$), 2.28 (t, 2 H, $CpCH_2$), 4.20 (s, 4 H, HCp), 4.58 (s, 2 H, HCp), 4.83 (s, 2 H, HCp).

***N*-(1′-Tetradecyl-1-acylferrocene)-1-amino-1-deoxy-D-sorbitol (1).** A solution of **6** (625 mg, 1.4 mmol) in CH_2Cl_2 (7 mL) was added dropwise to a hot (80 °C) solution of 1-amino-1-deoxy-D-sorbitol (2.6 g, 14.3 mmol) and DMAP (catalytic amount) in DMF (20 mL). The mixture was heated at 80 °C for 3 h and then kept at room temperature for 24 h. The mixture was filtered and evaporated to dryness. Purification of the solid residue by CC (CH_2Cl_2/MeOH 10:3 v/v) and crystallization (acetone) gave pure **1** (300 mg, 36%). ^{1}H NMR (400 MHz, $(CD_3)_2SO$) δ: 0.85 (t, 3 H, CH_3), 1.23 (m, 22 H, $(CH_2)_{11}$), 1.39 (m, 2 H, CH_2), 2.22 (t, 2 H, $CpCH_2$), 3.18, 3.39, 3.48, 3.58, 3.65, 3.71 (6 × m, 8 H, NCH_2, 4 × C*H*OH, CH_2-OH), 4.04 (s, 4 H, HCp), 4.26 (s, 2 H, HCp), 4.33 (d, 1 H, OH), 4.36 (d, 1 H, OH), 4.45 (d, 1 H, OH), 4.47 (d, 1 H, OH), 4.69 (d, 2 H, HCp), 4.87 (d, 1 H, OH), 7.69 (t, 1 H, CONH). ^{13}C NMR (100 MHz, $(CD_3)_2SO$) δ: 14.05, 22.20, 28.09, 28.81, 29.01, 29.07, 29.12, 29.15, 30.64, 31.40, 42.35, 63.49, 68.63, 68.64, 68.74, 69.30, 69.33, 69.36, 70.52, 71.59, 72.42, 72.62, 76.88, 90.07, 169.62. IR(KBr) ν (cm^{-1}): 3546s (free OH); 3420sh (weakly bonded OH stretching); 3307brs, 3118s (NH stretching); 2958m, 2917s, 2874m, 2849s (chains CH stretching); 1611s (CO stretching); 1567s (NH bending). MS: 590.0 ($MH^{\bullet+}$), 612.0 ($MNa^{\bullet+}$) Anal. Calcd for $C_{31}H_{51}NO_6Fe$ (589.60): C, 63.15; H, 8.72; N, 2.38. Found: 63.17; H, 8.54; N, 2.34.

Acknowledgment. R.D. acknowledges Ciba-Geigy-Jubiläums-Stiftung for a fellowship to B.D. and the Swiss National Science Foundation for financial support.

OM0001568

(26) Raimondi, M. E.; Seddon, J. M. *Liq. Cryst.* **1999**, *26*, 305.
(27) Jervis, H. B.; Raimondi, M. E.; Raja, R.; Maschmeyer, T.; Seddon, J. M.; Bruce, D. W. *Chem. Commun.* **1999**, 2031.